Facile synthesis of graphene coupled silver nanostructure-based hybrid SERS for trace-level SERS detection of Thiram

Himani Bhatia[1,2], Kiran M Subhedar[1,2]*
[1]CSIR-National Physical Laboratory (NPL), New Delhi, 110 012, India
[2]Academy of Scientific and Innovative Research (AcSIR), Ghaziabad, 201 002, India
*E-mail: kmsubhedar@gmail.com and kms@nplindia.org

1. Finite-Difference Time-Domain (FDTD) Simulation Parameters

The FDTD simulations were carried out with a mesh resolution of 1 nm in all three directions, a plane wave periodic source, an excitation wavelength of 785 nm, and perfectly matched layer (PML) boundary conditions. The simulation region was set to 300 nm × 300 nm × 2000 nm.

For the hybrid AgNS/Gr model, graphene was treated as an analytical material with diagonal anisotropy in the FDTD framework. A global mesh size of 1 nm was used for the simulation domain, while a finer local mesh of 0.1 nm was applied in the graphene region to accurately represent the atomically thin layer.

2. SERS measurements and analysis

The Raman spectra were recorded from five distinct positions (S-1 to S-5) on the same AgNS-silicon substrate with 50 s deposition, using thiram at a concentration of 10^{-3} M. The measured intensities at the 1382 cm^{-1} Raman peak showed a mean value of 16,780.49 a.u. with a standard deviation of 158.53 a.u., corresponding to a relative standard deviation (RSD) of 0.94%, confirming consistent Raman signals across the sampled positions. As shown in Figure S1, the 3D-stacked spectra further illustrate the uniformity and reproducibility of the SERS response across the tested regions, supporting the reliability of the measurements.

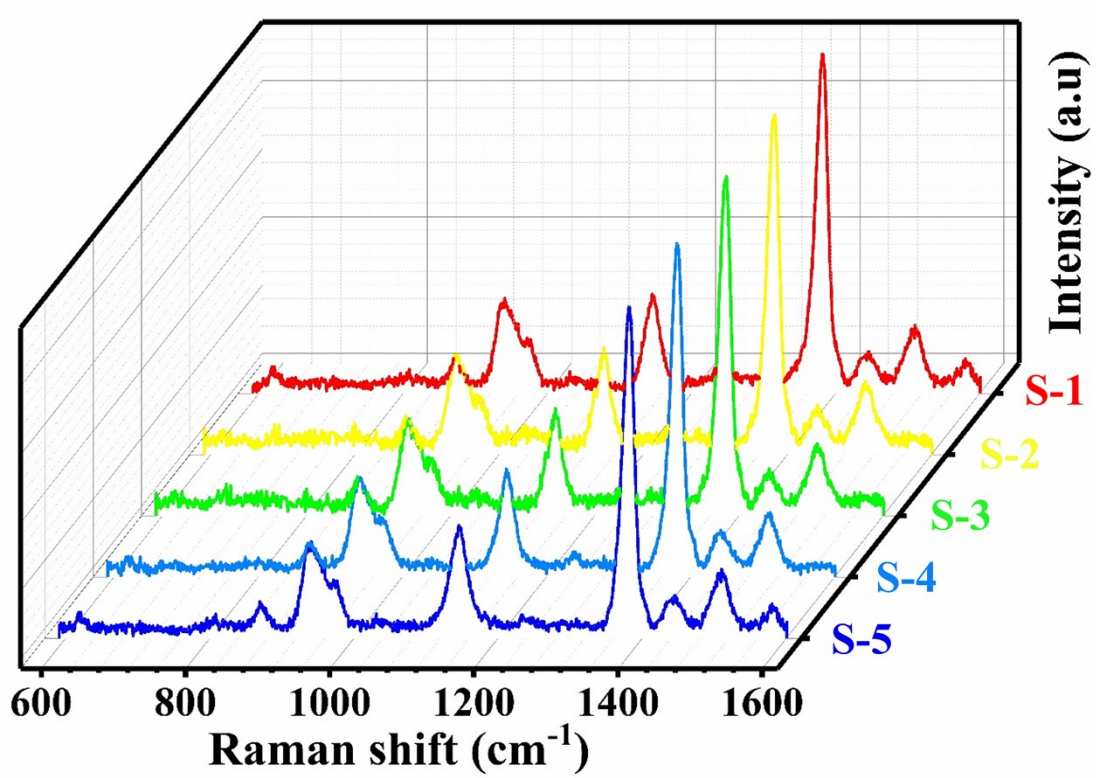

Figure S1: 3D-stacked Raman spectra from five positions on the same AgNS-silicon substrate (50 s deposition) at a fixed concentration of 10^{-3} M.

Raman measurements were conducted on a bare silicon substrate to assess the background contribution from the substrate and any residual PMMA from the graphene transfer. The spectrum of Thiram on bare silicon, shown in Supplementary Figure S2, indicates minimal background features, providing a reference for comparison with the signals obtained from the graphene-based hybrid substrate.

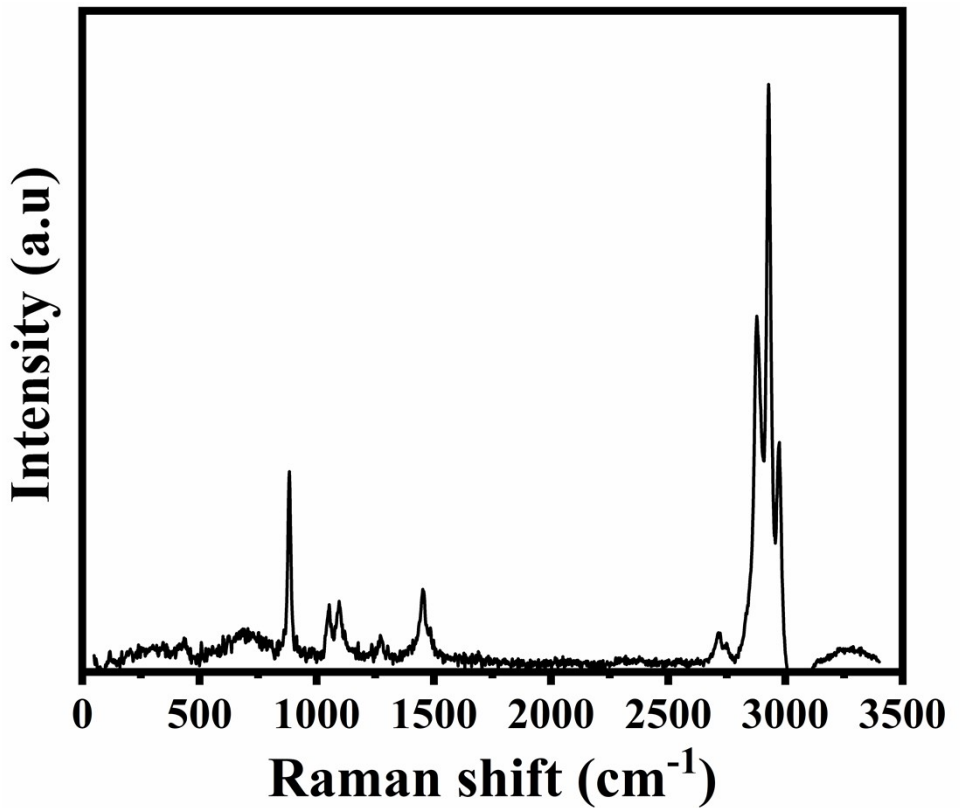

Figure S2: Raman spectrum of Thiram on a bare silicon substrate.

3. Effect of excitation wavelength on SERS performance

To inspect the correlation of the SERS activity with the plasmon resonance response of the AgNS, the lasers with two different wavelengths of 514 and 785 nm were used for the SERS detection of thiram. It was found that the 785 nm laser induced distinct characteristic peaks in the SERS spectrum of thiram, which were not observed in the 514 nm spectrum, as shown in Figure S3, indicating that when the Raman excitation laser wavelength is consistent with the LSPR band, the AgNS shows the strongest SERS responses.

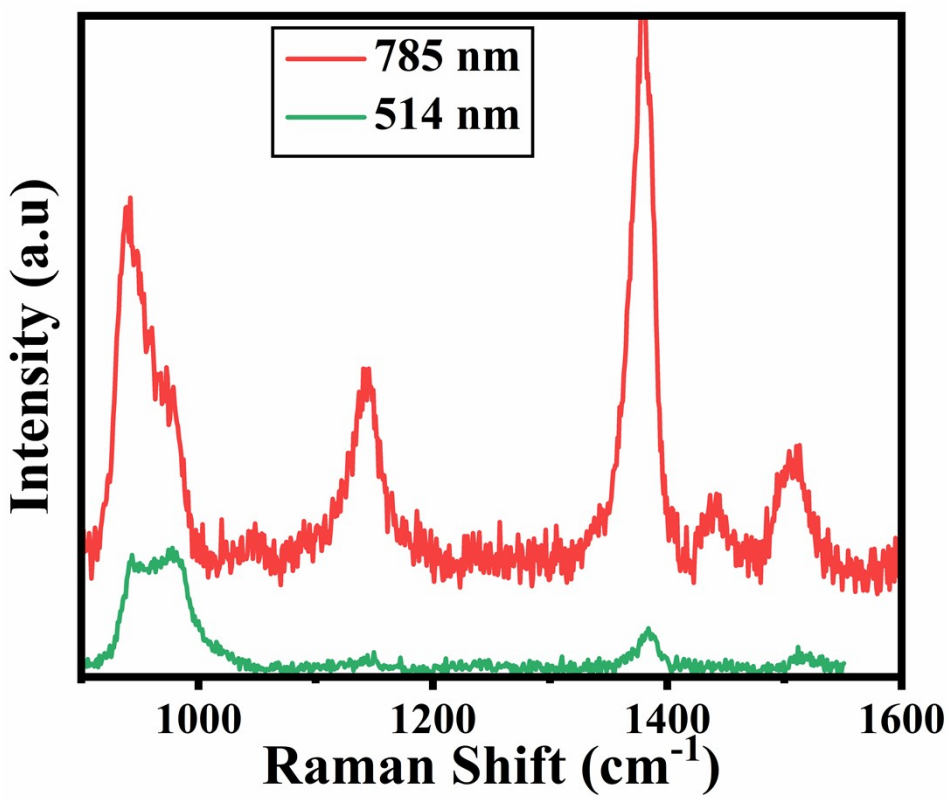

Figure S3: SERS spectra of 10^{-3} M thiram obtained from the AgNS using an excitation laser with wavelengths of 785 nm and 514 nm.

4. Role of the placement of HOMO-LUMO Energy Levels on SERS Signal

The SERS measurements were carried out using a 785 nm laser excitation, corresponding to a calculated laser energy (E) of 1.58 eV, determined via the well-established relation

$$E = \frac{hc}{\lambda} \quad (1),$$

where λ denotes the wavelength, c is the speed of light in a vacuum, and h represents Planck's constant. The electrochemical data revealed that the HOMO-LUMO energy gaps of thiram were 3.19 eV, respectively, providing valuable insights into their electronic properties. It is evident that the incident laser energy was insufficient to induce a resonance condition. The Chemical Enhancement mechanism (CM) involves the relaxation of electrons from the LUMO to the HOMO levels of the analyte adsorbed on a metal surface, resulting in the emission of Raman signals. However, this mechanism is considered the weakest, contributing an enhancement factor of approximately 10-100 times, which represents only a minor portion of the substantial Raman intensity enhancement observed in the SERS effect [1]. Consequently,

this contribution alone is not adequate to account for the significant differences in the trace level detection of thiram. Instead, the dominant mechanism involves both chemical (CM) and electromagnetic (EM) effects, with the surface plasmon resonance (SPR)-induced hot-electron transfer, commonly referred to as charge transfer (CT), playing a pivotal role.

Figure S4 illustrates three potential CT possibilities between the graphene and the adsorbed molecule: (a) when the Fermi level (E_F) of the graphene exceeds the HOMO energy level of the analyte (Figure S4a); (b) when E_F is lying in between HOMO and LUMO energy levels of the analyte (Figure S4b); and (c) when E_F is less than the LUMO energy level of the analyte (Figure S4c). Otero et al. proposed that electron transfer between the metal and the analyte, whether from the metal to the analyte or vice versa, can occur even in the absence of laser excitation in two cases: $E_F < E_{LUMO}$ and $E_F > E_{HOMO}$ [2].

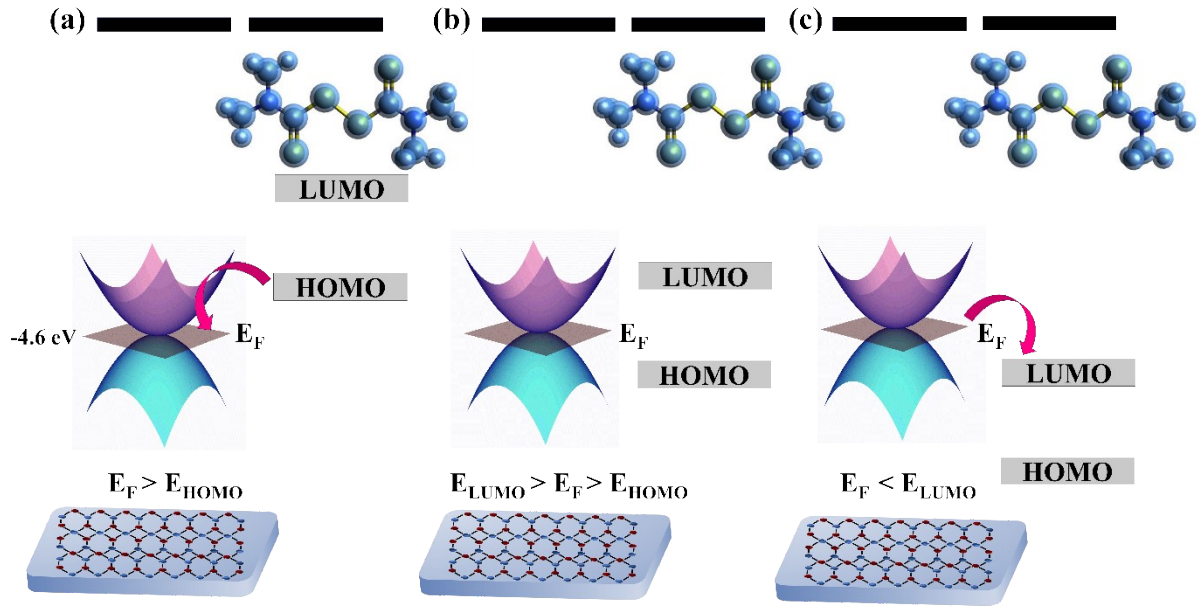

Figure S4: Schematic representation of the relative positioning of E_F of graphene (left) and the HOMO-LUMO energy levels of the Thiram analyte (right) is shown for three distinct cases: (a) $E_F > E_{HOMO,}$ (b) $E_{HOMO} > E_F > E_{LUMO,}$ and (c) $E_F < E_{LUMO}$.

5. Stability of AgNS/Gr substrates under ambient air conditions

To evaluate the stability of the AgNS/Gr substrates under ambient air exposure, Raman spectra of thiram (10^{-3} M) were recorded after storage in air for 1, 2, and 4 weeks. All measurements were performed under identical experimental conditions. As shown in Figure S5, the characteristic Raman features of thiram decrease with increasing air-exposure time, indicating a progressive loss of SERS activity upon prolonged storage in ambient air.

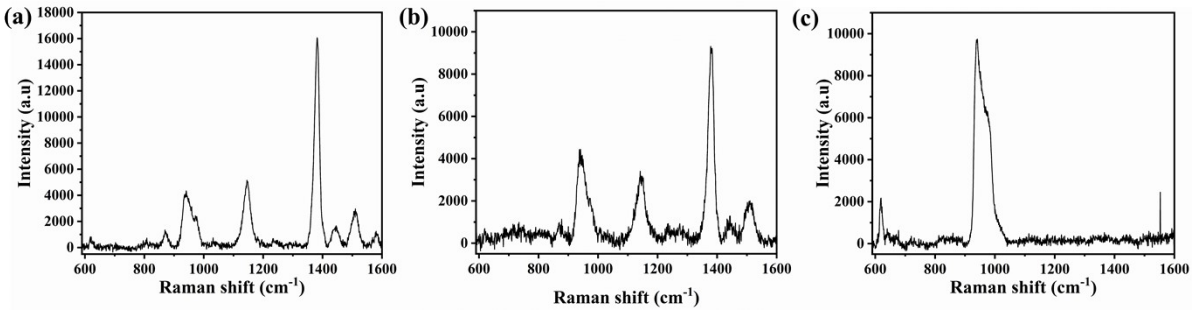

Figure S5: Raman spectra of thiram (10^{-3} M) recorded using AgNS/Gr substrates after storage under ambient air conditions for (a) 1 week, (b) 2 weeks, and (c) 4 weeks, measured under identical experimental conditions.

References:

[1] S.M. Morton, D.W. Silverstein, L. Jensen, Theoretical studies of plasmonics using electronic structure methods. Chemical reviews, 111 (2011) 3962-3994.
[2] R. Otero, A.V. de Parga, J.M. Gallego, Electronic, structural and chemical effects of charge-transfer at organic/inorganic interfaces. Surface Science Reports, 72 (2017) 105-145.